Inhomogeneous screening near the dielectric interface

Rui Wang and Zhen-Gang Wang

Citation: The Journal of Chemical Physics **144**, 134902 (2016); doi: 10.1063/1.4945011
View online: http://dx.doi.org/10.1063/1.4945011
View Table of Contents: http://scitation.aip.org/content/aip/journal/jcp/144/13?ver=pdfcov
Published by the AIP Publishing

Inhomogeneous screening near the dielectric interface

Rui Wang and Zhen-Gang Wang[a)]
Division of Chemistry and Chemical Engineering, California Institute of Technology, Pasadena, California 91125, USA

(Received 18 November 2015; accepted 18 March 2016; published online 5 April 2016)

Screening is one of the most important concepts in the study of charged systems. Near a dielectric interface, the ion distribution in a salt solution can be highly nonuniform. Here, we develop a theory that self-consistently treats the inhomogeneous screening effects. At higher concentrations when the bulk Debye screening length is comparable to the Bjerrum length, the double layer structure and interfacial properties are significantly affected by the inhomogeneous screening. In particular, the depletion zone is considerably wider than that predicted by the bulk screening approximation or the WKB approximation. The characteristic length of the depletion layer in this regime scales with the Bjerrum length, resulting in a linear increase of the negative adsorption of ions with concentration, in agreement with experiments. For asymmetric salts, inhomogeneous screening leads to enhanced charge separation and surface potential. © *2016 AIP Publishing LLC.* [http://dx.doi.org/10.1063/1.4945011]

I. INTRODUCTION

Screening due to the ionic atmosphere is one of the most important concepts in electrostatics.[1–7] The concept was introduced 90 yr ago by Debye and Hückel in the study of the thermodynamic properties of bulk electrolyte solution,[8] who showed that the bare $1/r$ Coulomb interaction becomes damped exponentially with a screening length κ_b^{-1}. Screening has profound effects on essentially all properties in systems containing salt ions. Indeed, the effects of salts on the structure, thermodynamics and interfacial properties of soft-matter and biophysical systems are primarily due to screening. When the ion distribution is nonuniform, as in the vicinity of a charged surface or an interface with dielectric discontinuity, screening also becomes inhomogeneous. The inhomogeneous screening of the fixed surface charge by the mobile ions is accounted for, at the mean-field level, by the Poisson-Boltzmann theory;[1–3] however, the inhomogeneous screening of the charge on a mobile ion, manifested by its interactions with other mobile ions as well as with its own image charge, has not been fully examined.

For a salt solution near a dielectric interface, e.g., the water/air interface, the repulsive image force creates a depletion layer, whose theoretical treatment was pioneered by Onsager and Samaras (OS)[9] based on the work of Wagner.[10] This problem is related to a number of phenomena, such as conductivity in artificial and biological ion-channels,[11–14] stability of colloidal, bubble, and protein suspensions,[15–18] and the rate of ozone consumption.[19,20] Assuming that the image force is screened by the bulk Debye length, the OS theory qualitatively explains the excess surface tension of the electrolyte solution observed in experiments and yields agreement with the experiment data in the low salt concentration regime ($c_b < 0.01$M). However, there is large discrepancy between the OS theory prediction and experimental data at high salt concentrations ($c_b > 0.1$M).[21,22] The OS theory predicts that the width of the depletion layer shrinks as the salt concentration increases, which results in a concave downwards curve for surface tension vs. c_b. In contrast, the experimental data show essentially a linear increase of the surface tension with the salt concentration for $c_b > 0.1$M. To reconcile the discrepancy with the experiment data, an exclusion zone of constant width or large hydrated radius of the ions is usually invoked in recent theoretical descriptions.[23,24]

An obvious effect missing in the OS theory[9] and in subsequent modifications[23–39] is the spatially varying screening of the image force near a dielectric interface (see Figure 1): the ion concentration changes gradually from zero at the interface to the bulk value. In this depletion layer, the ionic cloud is highly anisotropic, giving rise to different features of the screening near the interface from the homogeneous and isotropic bulk. Close to the interface, ions are strongly depleted; the local ionic strength around the test ion (Ion 1 in Figure 1) is much lower than the bulk. The bulk screening approximation clearly overestimates the screening effect and hence underestimates the image force. Even for an ion approaching the bulk (Ion 2 in Figure 1), the screening is still weaker than in the bulk due to the long-range, accumulative effects from the depletion zone. This feature extends the effective range of the image force beyond the Debye screening length. The WKB approximation[37,38] provides an approximate treatment of the inhomogeneous nature of screening by using the local ionic strength; however, it does not capture the long-range, accumulative effects.

Since approximate treatments cannot fully account for all the features of inhomogeneous screening, previous calculations using these approximations for the double layer structure and interfacial properties are likely to be inaccurate. Such inaccuracy in treating the essential electrostatic contributions makes it impossible to evaluate the relative importance of the various non-electrostatic effects invoked,

a)zgw@caltech.edu

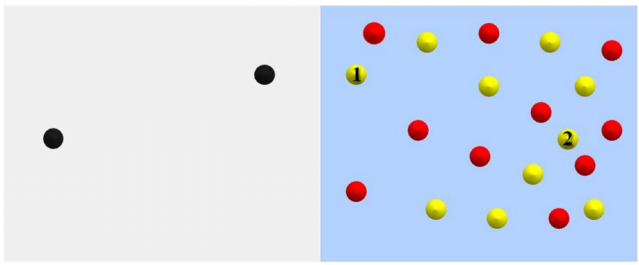

FIG. 1. Schematic of the inhomogeneous screening near the dielectric interface. The red and yellow spheres represent the cations and anions, respectively. The two test ions are labeled, with Ion 1 located very close to the interface and Ion 2 approaching the bulk solution. The two black spheres are the image charges corresponding to the two test ions.

for example, to explain the surface tension behavior, such as the cavity energy,[23,24] hydration,[24] and dispersion forces.[27,28] In this work, we examine the issue of inhomogeneous screening in salt solutions near a dielectric interface using a nonperturbative fluctuation theory developed by us.[40–42] By comparing the result from numerical solution of the full Green function with results obtained using approximate methods, we find that the effects of inhomogeneous screening on the double layer structure and interfacial properties are quite pronounced as the Debye screening length becomes comparable to the Bjerrum length.

II. THEORY

In recent work, we have shown that the image charge repulsion generates a depletion boundary layer near the dielectric interface, which necessitates a non-perturbative treatment.[42] Using a renormalized Gaussian variational approach,[43] we developed a general theory for weak-coupling systems with a fixed charge distribution $\rho_{ex}(\mathbf{r})$ in the presence of mobile cations with charge q_+e and anions with charge q_-e, in a dielectric medium of a spatially varying dielectric function $\varepsilon(\mathbf{r})$.[40] The key result of the theory is the following set of self-consistent equations for the mean electrostatic potential $\psi(\mathbf{r})$ (nondimensionalized by kT/e), the correlation function (Green function) $G(\mathbf{r},\mathbf{r}')$, and the self-energy $u_\pm(\mathbf{r})$ of the mobile ions

$$-\nabla\cdot(\epsilon\nabla\psi) = \rho_{ex} + \Gamma\lambda_+ q_+ e^{-q_+\psi-u_+} - \Gamma\lambda_- q_- e^{q_-\psi-u_-}, \quad (2.1)$$

$$-\nabla\cdot[\epsilon\nabla G(\mathbf{r},\mathbf{r}')] + 2I(\mathbf{r})G(\mathbf{r},\mathbf{r}') = \delta(\mathbf{r}-\mathbf{r}'), \quad (2.2)$$

$$u_\pm(\mathbf{r}) = \frac{1}{2}\int d\mathbf{r}'d\mathbf{r}''h_\pm(\mathbf{r}-\mathbf{r}')G(\mathbf{r}',\mathbf{r}'')h_\pm(\mathbf{r}''-\mathbf{r}). \quad (2.3)$$

In these equations, ϵ is the scaled permittivity $\epsilon = kT\varepsilon_0\varepsilon(\mathbf{r})/e^2$. $\lambda_\pm$ is the fugacity of cations and anions determined from the bulk salt concentration. The function $\Gamma(\mathbf{r})$ is introduced to constrain the mobile ions in the solvent region; $\Gamma = 1$ in the solvent region and $\Gamma = 0$ in regions inaccessible to the mobiles. $I(\mathbf{r}) = \left[q_+^2 c_+(\mathbf{r}) + q_-^2 c_-(\mathbf{r})\right]/2$ is the local ionic strength, with the concentration of cations and anions given by

$$c_\pm(\mathbf{r}) = \lambda_\pm\Gamma\exp\left[\mp q_\pm\psi(\mathbf{r}) - u_\pm(\mathbf{r})\right]. \quad (2.4)$$

The short-range charge distribution function $h_\pm(\mathbf{r}-\mathbf{r}')$ on the ion in Eq. (2.3) is introduced to yield a finite Born solvation energy. For our purpose, we will eventually take the point-charge limit $h_\pm(\mathbf{r}-\mathbf{r}') = q_\pm\delta(\mathbf{r}-\mathbf{r}')$.

Eq. (2.1) is the self-energy modified Poisson-Boltzmann (PB) equation, reflecting the fact that the ion distribution is determined by both the mean electrostatic potential and the self-energy. The Green function in Eq. (2.2) is a conditional potential at $\mathbf{r}$ generated by a point charge at $\mathbf{r}'$ mediated by other mobile ions, in the presence of spatially varying dielectric constant and ionic strength. The self-energy given by Eq. (2.3) is a unified expression that includes the Born energy of the ion, the interaction between the ion and its ionic atmosphere, as well as the image charge interaction. As shown in Eqs. (2.2) and (2.3), the inhomogeneity in the ionic strength affects the solution of the Green function and the self-energy, which consequently affect the double layer structure through Eq. (2.1), especially when the fixed charge density is small.

The set of Equations (2.1)–(2.4) are applicable to arbitrary geometry and fixed charge distribution. We now specify to a salt solution in contact with a low dielectric medium through a sharp interface (at $z = 0$) with fixed surface charge density $\rho_{ex}(\mathbf{r}) = \sigma\delta(z)$. Mobile ions are excluded from the low dielectric side. Both Γ and ε are then step functions: $\Gamma = 0$ and $\varepsilon = \varepsilon_P$ for $z < 0$;[44] $\Gamma = 1$ and $\varepsilon = \varepsilon_S$ for $z > 0$. In the solvent region ($z > 0$), Eq. (2.1) becomes

$$-\epsilon_S\frac{\partial^2\psi(z)}{\partial z^2} = \lambda_+ q_+ e^{-q_+\psi-u_+} - \lambda_- q_- e^{q_-\psi-u_-}, \quad (2.5)$$

with boundary condition $(\partial\psi/\partial z)_{z=0} = -\sigma/\epsilon_S$.

Assuming the solvent has a uniform dielectric constant in the entire $z > 0$ region, the Born energy is constant and can be absorbed into the reference chemical potential. We single out this constant contribution by rewriting Eq. (2.3) as

$$u_\pm(\mathbf{r}) = \frac{1}{2}\int d\mathbf{r}'d\mathbf{r}''h_\pm(\mathbf{r}-\mathbf{r}')\frac{1}{4\pi\epsilon_S|\mathbf{r}'-\mathbf{r}''|}h_\pm(\mathbf{r}''-\mathbf{r}) + \frac{1}{2}\int d\mathbf{r}'d\mathbf{r}''h_\pm(\mathbf{r}-\mathbf{r}') \times\left[G(\mathbf{r}',\mathbf{r}'') - \frac{1}{4\pi\epsilon_S|\mathbf{r}'-\mathbf{r}''|}\right]h_\pm(\mathbf{r}''-\mathbf{r}), \quad (2.6)$$

where we recognize the first term on the right hand side as the Born energy. The remaining contribution is finite in the point-charge limit, so we can simply set $h_\pm(\mathbf{r}-\mathbf{r}') = q_\pm\delta(\mathbf{r}-\mathbf{r}')$, which leads to the following expression for the nontrivial and nondivergent part of the self-energy $u_\pm^*$:

$$u_\pm^* = \frac{q_\pm^2}{2}\lim_{\mathbf{r}'\to\mathbf{r}}\left[G(\mathbf{r},\mathbf{r}') - \frac{1}{4\pi\epsilon_S|\mathbf{r}-\mathbf{r}'|}\right]. \quad (2.7)$$

To solve the Green function in the planar geometry, it is convenient to use a cylindrical coordinate (r,z). Owing to the translational invariance in the directions parallel to the interface, the Green function is most conveniently expressed using a partial Fourier transform in the transverse directions

$$G(r,z,z') = \frac{1}{2\pi}\int_0^\infty kdkJ_0(kr)\hat{G}(k,z,z'), \quad (2.8)$$

where J_0 is the zeroth-order Bessel function. It is easy to show that $\hat{G}(k,z,z')$ satisfies

$$-\frac{\partial^2\hat{G}(k,z,z')}{\partial z^2}+\left[\kappa^2(z)+k^2\right]\hat{G}(k,z,z')=\frac{1}{\epsilon_S}\delta(z,z'), \quad (2.9)$$

for $z>0$, with the boundary condition $\epsilon_S\partial\hat{G}/\partial z-k\epsilon_P\hat{G}=0$ at $z=0$. This boundary condition is obtained by combining the continuity of $\hat{G}(k,z,z')$ at $z=0$ with the form of the analytical solution for $\hat{G}(k,z,z')$ in the $z<0$ region. $\kappa(z)=[2I(z)/\epsilon_S]^{1/2}$ can be considered the inverse of the local Debye screening length.

Two approximate approaches are usually adopted in the literature to avoid numerically solving the high-dimensional Green function. The simplest and most common approximation is the bulk screening approximation,[9,23–35] which replaces the spatially varying screening length $\kappa(z)$ in Eq. (2.9) by the constant bulk screening length κ_b. With the bulk screening approximation, the Green function has an analytical solution as

$$\hat{G}(k,z,z')=\frac{1}{2\epsilon_S\omega}\left[\mathrm{e}^{-\omega|z-z'|}+\Delta\mathrm{e}^{-\omega(z+z')}\right], \quad (2.10)$$

where $\omega=\sqrt{\kappa_b^2+k^2}$ and $\Delta=(\epsilon_S\omega-\epsilon_Pk)/(\epsilon_S\omega+\epsilon_Pk)$. Substituting Eq. (2.10) into Eq. (2.8) leads to the following intuitive form for the self-energy when $\epsilon_S\gg\epsilon_P$:

$$u_\pm^*=\frac{q_\pm^2}{8\pi\epsilon_S}\left(-\kappa_b+\frac{f\mathrm{e}^{-2\kappa_bz}}{2z}\right), \quad (2.11)$$

with $f=(\epsilon_S-\epsilon_P)/(\epsilon_S+\epsilon_P)$ denoting the dielectric contrast. The first term on the right hand side of Eq. (2.11) accounts for the interaction with the local ionic atmosphere surrounding the test ion, and the second term is the image-charge interaction, which is repulsive for $f>0$. The second approximate approach was proposed by Buff and Stillinger based on the WKB approximation:[37,38,41] the Green function is first solved for a constant ionic strength, but in the resulting expression (Eq. (2.11)) the bulk κ_b is replaced by its local value $\kappa(z)=[2I(z)/\epsilon_S]^{1/2}$ that depends on the local, spatially dependent ionic strength $I(z)$.

In this work, we perform the full numerical calculation of the Green function using the finite difference method.[45] For each k, Eq. (2.9) is solved with 2000 grid points for the variable z and 20 000 grid points for the variable z'. We use different discretization between z and z' to increase the numerical accuracy in calculating the self-energy for the ions very close to the interface. The Dirac delta function is approximated by the Kronecker delta. In order to ensure consistent numerical accuracy in removing the singular part of the same-point Green function, the free-space Green function satisfying $-\partial^2\hat{G}_0/\partial z^2+k^2\hat{G}_0=\delta(z,z')/\epsilon_S$ is also solved numerically along with Eq. (2.9). We obtain the following nontrivial and nondivergent part of the self-energy:

$$u_\pm^*(z)=\frac{q_\pm^2}{4\pi}\int_0^\infty\left[\hat{G}(k,z,z)-\hat{G}_0(k,z,z)\right]kdk. \quad (2.12)$$

Numerical integration in the k space (Eq. (2.12)) is performed using the Simpson method with 200 grid points. Far away from the interface ($z\to\infty$), the ion concentration approaches the bulk value $c_\pm^b$. It is straightforward to show $\lambda_\pm=c_\pm^b\exp\left[-q_\pm^2\kappa_b/(8\pi\epsilon_S)\right]$.[40]

III. NUMERICAL RESULTS AND DISCUSSIONS

We now apply the theory to salt solutions near the water/air interface ($\varepsilon_S=80$ and $\varepsilon_P=1$) with zero fixed surface charge ($\sigma=0$). This is the same system studied by Onsager and Samaras. We first study salt solutions with equal-valent cations and anions, in which there is no charge separation and the electrostatic potential is everywhere zero. Then we study systems containing asymmetric salt, where different image force between cations and anions induces charge separation and hence a finite electric field. We compare the results from fully solving the Green function with results obtained by the bulk screening approximation and the WKB approximation. We note that the point-charge ions and the sharp interface represent a highly idealized model for the actual salt solutions near the water/air interface, where the ions have finite sizes and the interfacial width is comparable to the ion sizes. This simple model has been used in most of the literature that studies the same system. Here, we also use the same model to illustrate the concept of inhomogeneous screening and to provide comparison with previous approaches. Models with a finite charge distribution on the ion near a diffuse interface can be treated by our full theory (Equations (2.1)–(2.4)) without any essential difficulty.

The image charge repulsion creates a depletion boundary layer near the dielectric interface. In the absence of fixed surface charge, the structure of the depletion layer is governed by two length scales: the Bjerrum length $l_B=1/(4\pi\epsilon_S)$ (approximately 7 Å for water) and the bulk Debye screening length κ_b^{-1}. Within the Bjerrum length, the ion is strongly repelled by its own image charge; whereas beyond the bulk Debye screening length, the image charge repulsion is significantly reduced due to the screening from other ions. The effect of inhomogeneous screening on the ion distribution is twofold. First, within the Bjerrum length from the interface, there is little screening of the image-charge repulsion, and as a result, the depletion of ions on this length scale is stronger than predicted by the bulk screening-length approximation. Second, the low ion concentration near the interface has a long-range and accumulative effect on the screening strength beyond the Bjerrum length, which extends the range of the depletion layer. Figures 2(a) and 2(b) show the concentration profile of the ions in a 1:1 salt solution for two bulk concentrations. At low salt concentrations when $\kappa_b^{-1}\gg q^2l_B$, the effect of inhomogeneous screening is insignificant as shown in Figure 2(a), because screening is weak even in the bulk. In addition, in this regime, the accumulative effect of strong ion depletion within the Bjerrum length is relatively short-ranged compared to the Debye screening length. The behavior of the double layer is primarily characterized by the bulk Debye screening length. Both the bulk screening approximation and the WKB approximation are valid in this regime.

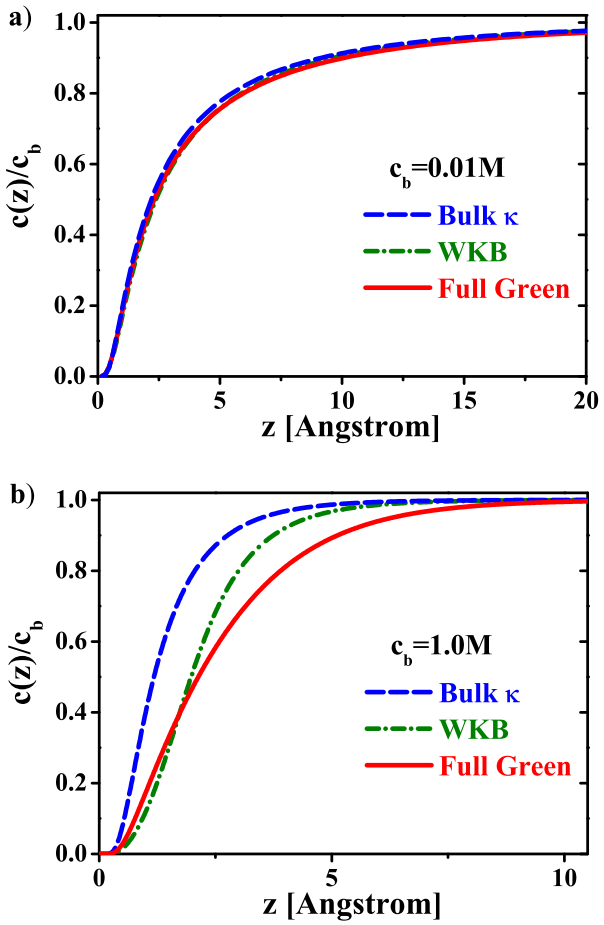

FIG. 2. Effect of inhomogeneous screening on the ion distribution of (a) 0.01M and (b) 1.0M 1:1 salt solution near the water/air interface. "Bulk κ", "WKB" and "Full Green" refer to the bulk screening approximation, the WKB approximation and numerically solving the full Green function, respectively.

In contrast, at higher salt concentrations when κ_b^{-1} becomes comparable to or even smaller than l_B; inhomogeneous screening affects the entire range of the depletion layer as shown in Figure 2(b). Close to the interface ($z < l_B$), the ion concentration calculated by fully solving the Green function is significantly lower than that predicted by the bulk screening approximation, because the local ionic strength is obviously smaller than the bulk. In Figures 3(a) and 3(b) we provide a more visual representation of inhomogeneous screening by plotting the nondivergent part of the Green function, $G(\mathbf{r},\mathbf{r}') - 1/(4\pi\epsilon_S|\mathbf{r}-\mathbf{r}'|)$, i.e., the nondivergent part of the linear response electrostatic potential generated by a test point charge at a given distance from the interface. The potential generated by the ion close to the interface ($z = 1.5$ Å) is much stronger than that predicted by the bulk screening approximation, the latter severely overestimating the local screening effect on the image charge interaction. Although this local effect is captured by the WKB approximation, neither of these two approximations capture the long-range and accumulative nature of the screening. The depletion layer calculated by fully solving the Green function extends to a range significantly longer than the bulk Debye screening length. As shown in Figure 3(d), even for an ion approaching the bulk solution ($z = 5$ Å, which is larger than the bulk screening length of 3.3 Å), the electric field from its image charge is not screened out. This remaining image charge interaction in turn has a long-range and accumulative effect that reinforces the field at the position of the point charge.

Levine and Bell suggested that the WKB approximation should provide the lower bound for the screening strength,[38] i.e., the actual screening should be stronger than described by the WKB approximation. This suggestion is not supported by our results: WKB actually over-screens the image-charge repulsion in the longer-range part of the ion profile. Overall, both the bulk screening approximation and the WKB approximation overestimate the long-range part of the screening and underestimate its effect on the image-charge repulsion. The two approximate methods become progressively poorer as the salt concentration increases.

While our discussions here are for the simple model of point-charge and sharp interface, we show in the Appendix that ion profile remains essentially unchanged for the case of a diffuse interface, as long as the interfacial width is comparable to the ion sizes, a condition that is satisfied by most liquid/air interfaces far way from the critical point; see Figure 7(a). When the interfacial width is much larger than the ion sizes, the ion profile in the interfacial region will be quantitatively different from the profile obtained using the sharp interface model as shown in Figure 7(b). However, the discrepancy between the results obtained by fully solving the Green function and by using both the bulk screening approximation and the WKB approximation persists. We emphasize that the use of the point-charge and sharp interface model for salt solutions near the water/air interface is to highlight the effects of inhomogeneous screening. The quantitative aspects of our results will be modified as more realistic features are included, such as the excluded volume of the ions and the cavity energy.[2,24,46,47] Nevertheless, inhomogeneous screening remains an essential feature in treating electrostatic interactions in nonuniform systems.

Applying a Gibbs-like construction, we define $d = \int_0^\infty [c_b - c(z)]\,dz/c_b$ to characterize the width of the ion depletion layer, which is shown in Figure 4 as a function of the salt concentration. The two approximate methods predict d to be an ever decreasing function of c^b, determined by the bulk Debye screening length ($d \sim \kappa_b^{-1}$). In contrast, d calculated by fully solving the Green function deviates significantly from the results of the approximate methods as κ_b^{-1} becomes comparable to $q^2 l_B$ and reaches a constant value as c_b further increases up to 1M. Thus, at high salt concentrations the image-charge repulsion renormalized by the inhomogeneous screening creates a depletion layer of nearly constant width scaled by the Bjerrum length ($d \sim q^2 l_B$) instead of κ_b^{-1} and becomes nearly independent of the salt concentration.

As a consequence of the different behavior in the width of the depletion layer due to inhomogeneous screening, there is pronounced difference in the negative adsorption of ions ($-\Gamma = \int_0^\infty [c(z) - c_b]\,dz$) at the interface between results obtained by fully solving the Green function and those using the approximate methods as shown in Figure 5.

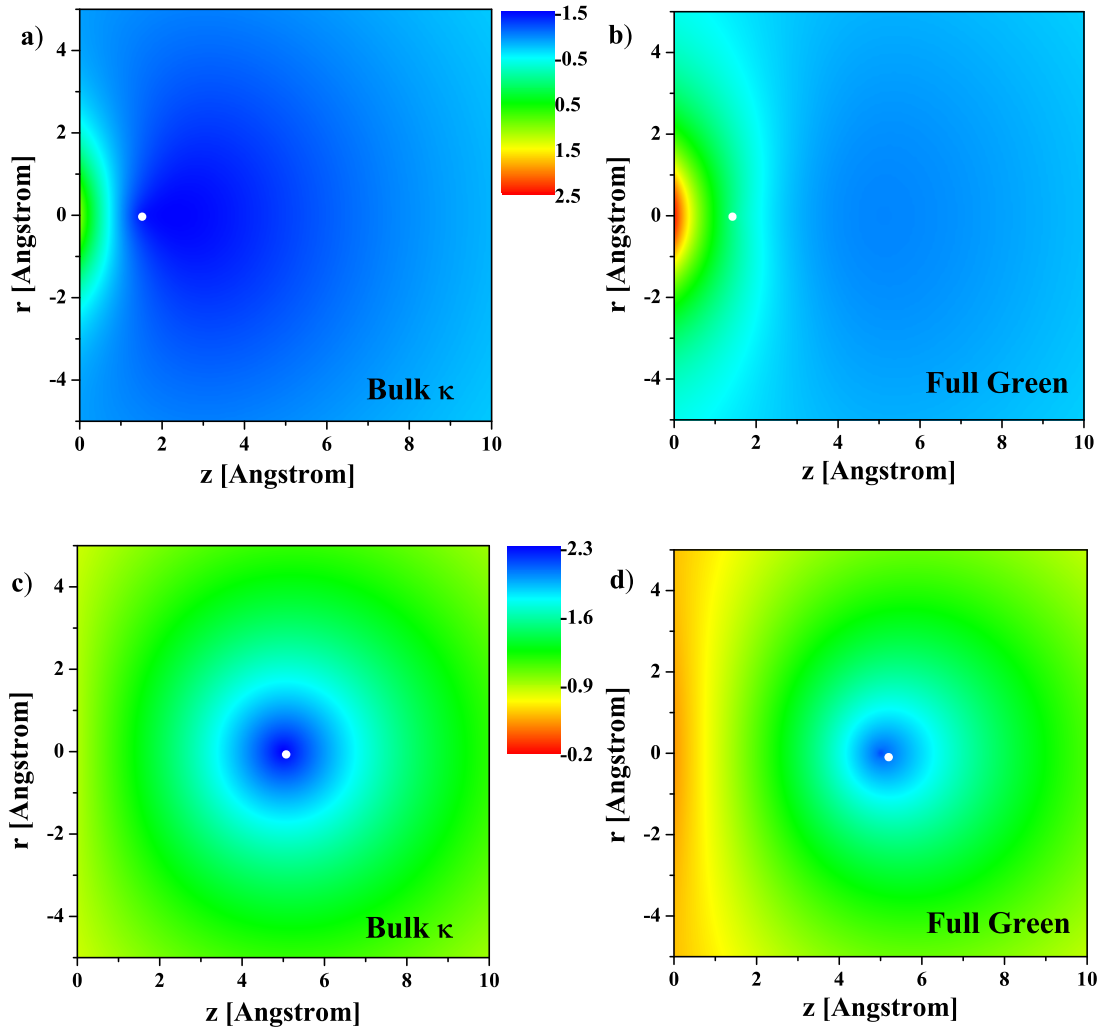

FIG. 3. 2D visualization of the nondivergent Green function, $G(\mathbf{r},\mathbf{r}') - 1/(4\pi\epsilon_S|\mathbf{r}-\mathbf{r}'|)$, for 1.0M 1:1 salt solution near the water/air interface. The test ion (white dot) is at $z' = 1.5$ Å for (a) and (b), and $z' = 5$ Å for (c) and (d).

Because the approximate methods predict an ever decreasing d as c_b increases, $-\Gamma$ is a concave downwards function of c_b, as first shown by Onsager and Samaras.[9] However, experimentally both $-\Gamma$ and the surface tension of the 1:1 salt solution increases essentially linearly with c_b in the range of 0.1M < c_b < 1M.[21,22] To fit the experimental data, an ion-exclusion zone with constant width has been invoked in previous theoretical treatments.[23,24] By fully accounting for

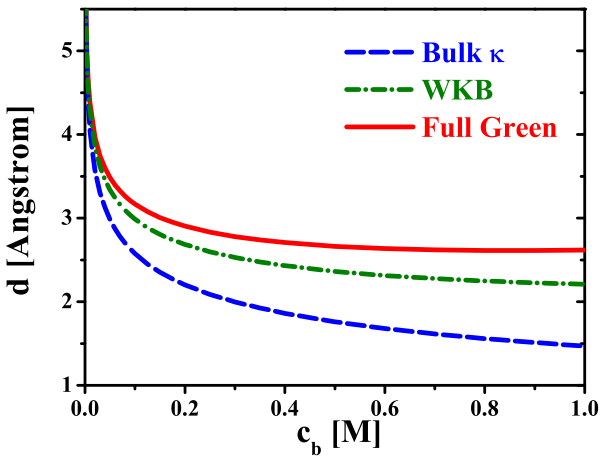

FIG. 4. The characteristic length of ion depletion as a function of salt concentration for a 1:1 salt solution at the water/air interface.

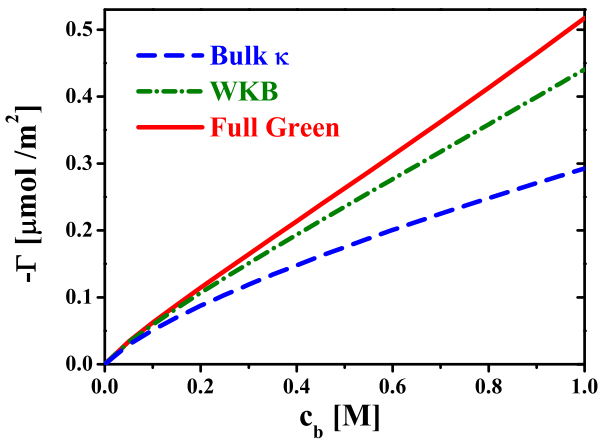

FIG. 5. Inhomogeneous screening effect on the negative adsorption of ions for a 1:1 salt solution at the water/air interface.

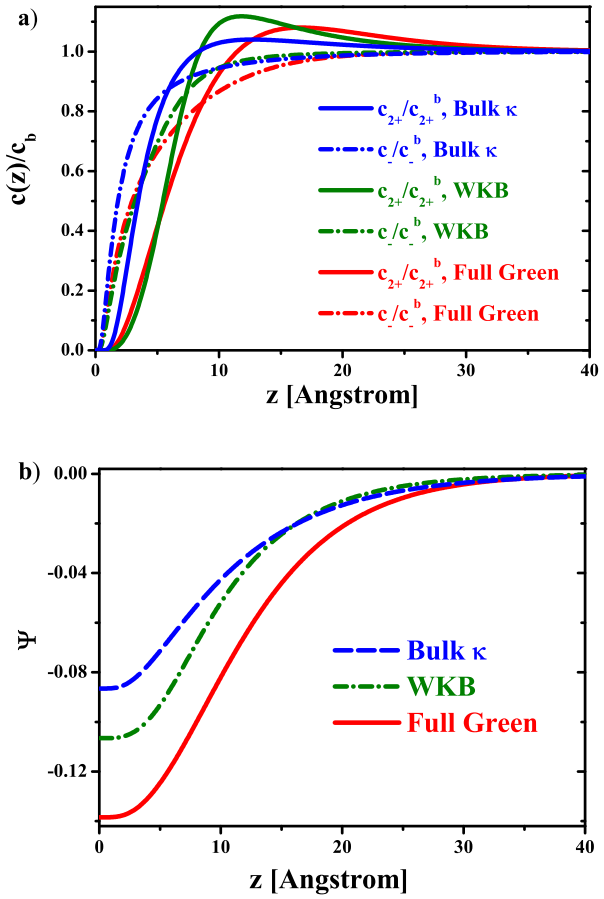

FIG. 6. Inhomogeneous screening effect on 0.05M 2:1 salt solution near the water/air interface. (a) Ion concentration scaled by $c_{\pm}^{b}$ and (b) dimensionless electrostatic potential.

the inhomogeneous screening, our theory naturally predicts that $-\Gamma$ increases linearly with c_b for $0.1\text{M} < c_b < 1\text{M}$, as a consequence of a nearly constant d. In light of these results, it is quite possible that the inhomogeneous screening of the image charge repulsion provides an explanation on the experimentally observed linear increase of the surface tension with the salt concentration; we are currently exploring this possibility.

Because of the quadratic dependence of the image-charge repulsion on the valency, in an asymmetric salt solution, multivalent ions will be more strongly depleted than monovalent ions. Furthermore, multivalent ions are more effective in screening. Therefore, inhomogeneous screening has an even more pronounced effect on asymmetric salt solutions containing multivalent ions. For a 2:1 salt solution, the divalent cations calculated by fully solving the Green function are pushed further away from the interface than predicted by the approximate methods as shown in Figure 6(a), leading to a larger degree of charge separation. As a result, the induced electrostatic potential is much larger than that obtained using the approximate methods; see Figure 6(b). Such a large self-induced surface potential can significantly affect the interpretation of the zeta potential of colloidal surfaces[1] and is a major contribution to the Jones-Ray effect in the surface tension of salt solution.[30,48–50]

IV. CONCLUSIONS

In this work, we have presented a self-consistent treatment of the inhomogeneous screening in salt solutions near a dielectric interface. The effect of inhomogeneous screening is twofold. First, the ionic atmosphere in the depletion layer is anisotropic with lower ionic strength than the bulk; this decreased ion concentration results in less screening on the image force and hence stronger ion depletion. Second, the ion depletion near the interface has a long-range and accumulative effect on screening, which extends the range of the depletion layer. Consequently, the ion distribution is significantly affected when the bulk screening length is comparable to or smaller than the Bjerrum length. In this regime, the depletion layer structure and the interfacial properties cannot be described by either the bulk screening approximation or the WKB approximation. The characteristic length of the depletion layer scales with the Bjerrum length, resulting in a linear increase of the negative adsorption of ions with concentration, in agreement with experiments. The inhomogeneous screening effect becomes more pronounced in less polar solvent and for ions of higher valency.

Nonuniform ion distribution near a dielectric interface exists in many colloidal and biophysical systems. Inhomogeneous screening is an integral part in the electrostatic contribution to the structure, thermodynamics and dynamics, which, however, has not been adequately treated in previous theoretical work. An accurate treatment of inhomogeneous screening is important to fully understand the role of electrostatic interactions in these systems, which in turn is necessary for evaluating the various nonelectrostatic contributions, such as the cavity energy, hydration, and dispersion forces to the surface and interface properties of aqueous solutions.[51–53] The relative importance of these nonelectrostatic contributions has been a subject of controversy.[54] In our opinion, the origin of the controversy reflects the lack of a uniform and accurate theory for treating the electrostatic contributions. By a more accurate treatment of the inhomogeneous screening effect, we are in a position to better evaluate the role nonelectrostatic contributions in the explanation of long standing problems, such as the specific ion effects and salt concentration effects in the water/air and water/oil interfacial tension.

ACKNOWLEDGMENTS

Acknowledgment is made to the donors of the American Chemical Society Petroleum Research Fund for partial support of this research.

APPENDIX: THE CASE OF A DIFFUSE INTERFACE

In this appendix, we present an approximate treatment of salt solutions near a diffuse water/air interface by combining the contributions from local Born solvation energy and the long-range image charge interaction. We will show that inhomogeneous screening persists when the interface has finite width.

We assume the following density profile (volume fraction $\phi(z)$) for water in the diffuse interface ($-\infty < z < \infty$) is set to be

$$\phi(z) = [1 + \tanh(z/\alpha)]/2, \tag{A1}$$

where the parameter α characterizes the width of the interface, and the Gibbs dividing interface is set at $z = 0$. The local dielectric constant is assumed to be a simple volume fraction weighted average of its two components,

$$\epsilon(z) = \epsilon_S \phi(z) + \epsilon_P [1 - \phi(z)]. \tag{A2}$$

Since the dielectric constant is spatially varying, the Born solvation energy is no longer constant. A finite charge distribution on the ion is necessary to avoid divergence of the Born energy in the point-charge model. However, numerically solving the full equations (Equations (2.1)–(2.4)) for ions with a finite charge distribution is nontrivial because both the small length-scale features on the scale of the ion radius and the large length-scale features on the scale of depletion layer need to be resolved.

Here, we use an approximate treatment by separating the self-energy of ions into a local contribution from Born solvation energy and long-range contributions that can be approximated using the point-charge model. Similarly to Eq. (2.7), we decompose the self-energy as

$$\begin{aligned} u_\pm(\mathbf{r}) = & \frac{1}{2}\int d\mathbf{r}' d\mathbf{r}'' h_\pm(\mathbf{r}-\mathbf{r}') G_0(\mathbf{r}',\mathbf{r}'') h_\pm(\mathbf{r}''-\mathbf{r}) \\ & + \frac{1}{2}\int d\mathbf{r}' d\mathbf{r}'' h_\pm(\mathbf{r}-\mathbf{r}') \\ & \times [G(\mathbf{r}',\mathbf{r}'') - G_0(\mathbf{r}',\mathbf{r}'')]\, h_\pm(\mathbf{r}''-\mathbf{r}), \end{aligned} \tag{A3}$$

where $G_0(\mathbf{r},\mathbf{r}')$ is now the free Green function in a spatially varying dielectric medium given by $-\nabla\cdot[\epsilon(z)\nabla G_0(\mathbf{r},\mathbf{r}')] = \delta(\mathbf{r}-\mathbf{r}')$. The first term on the right hand side of Eq. (A3) is Born solvation energy, which can be approximated by using the local dielectric constant as $q_\pm^2/[8\pi\epsilon(z)a_\pm]$,[40] with $a_\pm$ the Born radius of cations and anions. The second term on the right hand side of Eq. (A3) includes contributions from ion-ion correlation and image charge interaction, which is expected to be of longer range than the ion radius and hence can be approximated by using the point-charge model as in Eq. (2.12). Thus, Eq. (A3) is rewritten as

$$u_\pm(\mathbf{r}) \approx \frac{q_\pm^2}{8\pi\epsilon(z)a_\pm} + \frac{q_\pm^2}{4\pi}\int_0^\infty \left[\hat{G}(k,z,z) - \hat{G}_0(k,z,z)\right] k\,dk, \tag{A4}$$

where $\hat{G}(k,z,z')$ satisfies

$$\begin{aligned} & -\frac{\partial\epsilon(z)}{\partial z}\frac{\partial\hat{G}(k,z,z')}{\partial z} - \epsilon(z)\frac{\partial^2\hat{G}(k,z,z')}{\partial z^2} \\ & + \left[2I(z) + \epsilon(z)k^2\right]\hat{G}(k,z,z') = \delta(z,z'). \end{aligned} \tag{A5}$$

$\hat{G}_0(k,z,z')$ is a special case of $\hat{G}(k,z,z')$ with $I(z)$ in Eq. (A5) set to 0.

In Figure 7 we show the ion profiles calculated using the approximate treatment of the self-energy presented above. For interfacial widths comparable to the ion sizes (the case for most liquid/air interfaces far from critical point), the ion profiles are in good agreement with the profiles obtained for the sharp interface; see Figure 7(a). Our results presented in the main text using the sharp interface model is therefore quantitatively valid under such conditions. When the width of the interface is much larger than the ion size, the ion distribution is pushed towards the inner water region in comparison with the results obtained for the sharp interface; see Figure 7(b). However, inhomogeneous screening still persists in this case, as seen by the wider depletion layer obtained from fully solving the Green function in the diffuse interface compared with the results using bulk screening and WKB approximations.

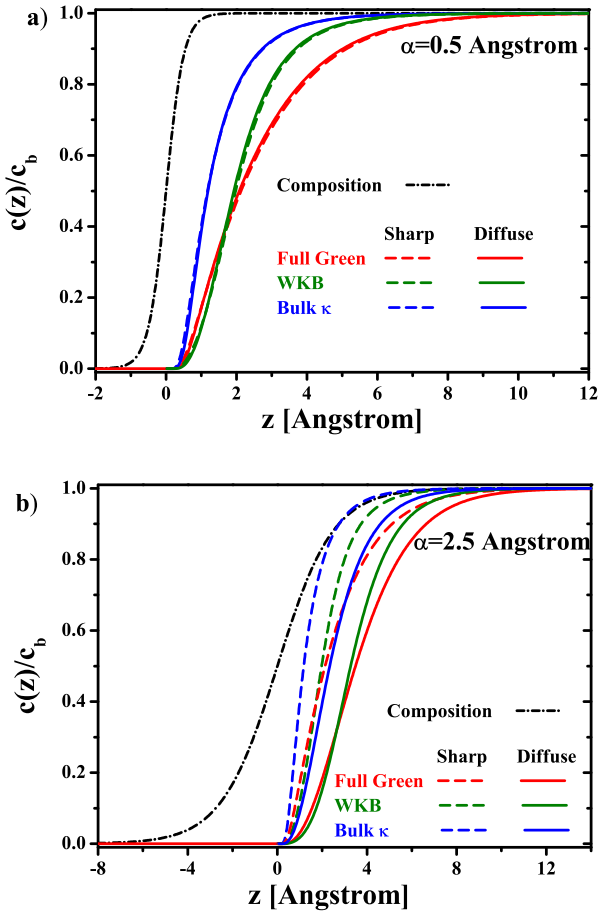

FIG. 7. Effect of inhomogeneous screening on the ion distribution of 1.0M 1:1 salt ($a_\pm = 1.0$ Å) solution near the water/air interface with diffuse composition profile as described in Eq. (A1). The ion profiles in the sharp interface are also shown for comparison. The width of diffuse interface in (a) is comparable to the ion sizes and in (b) much larger than the ion sizes and comparable to the Bjerrum length.

[1]J. N. Israelachvili, *Intermolecular and Surface Forces*, 2nd ed. (Academic, London, 1992).
[2]D. Andelman, in *Soft Condensed Matter Physics in Molecular and Cell Biology*, edited by W. C. K. Poon and D. Andelman (Taylor and Francis, Boca Raton, Florida, 2000).
[3]D. A. McQuarrie, *Statistical Mechanics* (University Science Books, Sausalito, California, 2000).
[4]Y. Levin, Rep. Prog. Phys. **65**, 1577 (2002).
[5]J. P. Hansen and H. Löwen, Annu. Rev. Phys. Chem. **51**, 209-242 (2000).
[6]B. Honig and A. Nicholls, Science **268**, 1144 (1995).
[7]M. Gelbart, R. F. Bruinsma, P. A. Pincus, and V. A. Parsegian, Phys. Today **53**(9), 38 (2000).
[8]P. Debye and E. Hückel, Phys. Z. **24**, 185 (1923).
[9]L. Onsager and N. N. T. Samaras, J. Chem. Phys. **2**, 528 (1933).
[10]C. Wagner, Phys. Z. **25**, 474 (1924).
[11]A. Parsegian, Nature **221**, 844 (1969).
[12]T. Bastug and S. Kuyucak, Biophys. J. **84**, 2871 (2003).
[13]S. Buyukdagli, M. Manghi, and J. Palmeri, Phys. Rev. Lett. **105**, 158103 (2010).

[14]E. D. Gomez, A. Panday, E. H. Feng, V. Chen, G. M. Stone, A. M. Minor, C. Kisielowski, K. H. Downing, O. Borodin, G. D. Smith, and N. P. Balsara, Nano Lett. **9**, 1212-1216 (2009).
[15]F. W. Tavares, D. Bratko, and J. M. Prausnitz, Curr. Opin. Colloid Interface Sci. **9**, 81 (2004).
[16]M. Gradzielski, Curr. Opin. Colloid Interface Sci. **9**, 256 (2004).
[17]V. S. J. Craig, B. W. Ninham, and R. M. Pashley, Nature **364**, 317 (1993).
[18]S. Kumar and R. Nussinov, Chembiochem **3**, 604 (2002).
[19]J. H. Hu, Q. Shi, P. Davidovits, D. R. Worsnop, M. S. Zahniser, and C. E. Kolb, J. Phys. Chem. **99**, 8768 (1995).
[20]E. M. Knipping, M. J. Lakin, K. L. Foster, P. Jungwirth, D. J. Tobias, R. B. Gerber, D. Dabdub, and B. J. Finlayson-Pitts, Science **288**, 301 (2000).
[21]N. Matubayasi, K. Yamamoto, S. Yamaguchi, H. Matsuo, and N. Ikeda, J. Colloid Interface Sci. **214**, 101 (1999).
[22]N. Matubayasi, K. Tsunemoto, I. Sato, R. Akizuki, T. Morishita, A. Matuzawa, and Y. Natsukari, J. Colloid Interface Sci. **243**, 444 (2001).
[23]Y. Levin and J. E. Flores-Mena, Europhys. Lett. **56**, 187 (2001).
[24]Y. Levin, A. P. dos Santos, and A. Diehl, Phys. Rev. Lett. **103**, 257802 (2009).
[25]A. Bakhshandeh, A. P. dos Santos, and Y. Levin, Phys. Rev. Lett. **107**, 107801 (2011).
[26]G. M. Bell and P. D. Rangecroft, Trans. Faraday Soc. **67**, 649 (1971).
[27]M. Boström, W. Kunz, and B. W. Ninham, Langmuir **21**, 2619 (2005).
[28]T. T. Duignan, D. F. Parsons, and B. W. Ninham, J. Phys. Chem. B **118**, 8700 (2014).
[29]A. Onuki, Phys. Rev. E **73**, 021506 (2006).
[30]A. Onuki, J. Chem. Phys. **128**, 224704 (2008).
[31]S. Buyukdagli, M. Manghi, and J. Palmeri, Phys. Rev. E **81**, 041601 (2010).
[32]D. S. Dean and R. R. Horgan, Phys. Rev. E **69**, 061603 (2004).
[33]R. Podgornik and B. Zeks, J. Chem. Soc., Faraday Trans. 2 **84**, 611 (1988).
[34]R. Podgornik, J. Chem. Phys. **91**, 5840-5849 (1989).
[35]T. Markovich, D. Andelman, and R. Podgornik, Europhys. Lett. **106**, 16002 (2014).
[36]J. W. Zwanikken and M. Olvera de la Cruz, Proc. Natl. Acad. Sci. U. S. A. **110**, 5301 (2013).
[37]F. P. Buff and F. H. Stillinger, J. Chem. Phys. **39**, 1911 (1963).
[38]G. M. Bell and S. Levine, J. Chem. Phys. **49**, 4584 (1968).
[39]C. W. Outhwaite and L. B. Bhuiyan, J. Chem. Soc., Faraday Trans. 2 **79**, 707-718 (1983).
[40]Z.-G. Wang, Phys. Rev. E **81**, 021501 (2010).
[41]R. Wang and Z.-G. Wang, J. Chem. Phys. **139**, 124702 (2013).
[42]R. Wang and Z.-G. Wang, J. Chem. Phys. **142**, 104705 (2015).
[43]R. R. Netz and H. Orland, Eur. Phys. J. E **11**, 301 (2003).
[44]When the low dielectric medium is not a solid, it is in principle accessible for mobile ions. However, for large dielectric contrast, as in the case of the air/water interface, the ion concentration in the low dielectric region will be exceedingly small due to the high Born energy penalty. To avoid dealing with such small numbers that are for all practical purposes inconsequential, it is more mathematically convenient to take the low dielectric medium as impenetrable for mobile ions by setting $\Gamma = 0$ for $z < 0$.
[45]Z. L. Xu, M. M. Ma, and P. Liu, Phys. Rev. E **90**, 013307 (2014).
[46]M. E. Fisher and Y. Levin, Phys. Rev. Lett. **71**, 3826 (1993).
[47]I. Borukhov, D. Andelman, and H. Orland, Phys. Rev. Lett. **79**, 435 (1997).
[48]G. Jones and W. A. Ray, J. Am. Chem. Soc. **59**, 187 (1937).
[49]M. Bier, J. Zwanikken, and R. van Roij, Phys. Rev. Lett. **101**, 046104 (2008).
[50]R. Wang and Z.-G. Wang, J. Chem. Phys. **135**, 014707 (2011).
[51]K. Lum, D. Chandler, and J. D. Weeks, J. Phys. Chem. B **103**, 4570 (2005); D. Chandler, Nature **437**, 640 (2005).
[52]S. Rajamani, T. M. Truskett, and S. Garde, Proc. Natl. Acad. Sci. U. S. A. **102**, 9475 (2005).
[53]M. Boström, D. R. M. Williams, and B. W. Ninham, Langmuir **17**, 4475 (2001).
[54]P. L. Nostro and B. W. Ninham, Chem. Rev. **112**, 2286 (2012).